

## Adhesion Force Mapping of Polymer Surfaces: Factors Influencing Force of Adhesion

Peter Eaton, James R. Smith, Paul Graham, John D. Smart, Thomas G. Nevell, and John Tsibouklis\*

School of Pharmacy and Biomedical Sciences, University of Portsmouth, St. Michael's Building, White Swan Road, Portsmouth PO1 2DT, U.K.

Received October 18, 2001. In Final Form: February 4, 2002

### Introduction

Nanoindentation measurements form the basis of an atomic force microscopy (AFM) technique that may be employed for the purpose of elucidating the surface heterogeneity of polymeric materials.<sup>1–9</sup> If the cantilever is stiffer than the substrate, measurement of the extent of cantilever deflection, as the tip is pressed into the sample, probes quantitatively the compliance of the surface as a function of applied load.<sup>10,11</sup> As with force-of-adhesion measurements, the quantification of indentation measurements may be impeded by the complexity of the tip–sample interactions, especially if a nonelastic surface is probed.<sup>12</sup>

In attempting to map the surface heterogeneity of a polymer sample, the spring constant of the AFM cantilever needs to be fine-tuned according to the demands of the probing technique. For a high signal-to-noise ratio, adhesion force measurements demand the use of a flexible cantilever<sup>13</sup> whereas indentation measurements require the use of stiff cantilevers such that the force applied to the sample is sufficient to indent the sample to a measurable extent. Furthermore, the AFM method of choice for the study of the surface heterogeneity of a polymeric sample is determined by the characteristics of that sample, as demonstrated by previous work with a poly(methyl methacrylate)/poly(dodecyl methacrylate) (PMMA/PDDMA) binary blend.<sup>5</sup> In this work, the adhesive forces that determine the extent of the interaction between the silicon nitride tip and the PDDMA-rich domains were seen to be markedly greater than corresponding forces operating between the same AFM tip and the harder,

PMMA-rich regions of the surface; in the absence of a surface-hardness calibration system, it was not possible to quantify the magnitude of the forces exerted on the tip by a unit area of PDDMA-rich or PMMA-rich surface. We now report on our efforts to bridge that gap by considering the effect of indentation on the measured forces that determine the adhesive interactions between an AFM tip and the surfaces of the same polymeric materials. Furthermore, we explore the complementarity of the techniques of adhesion force mapping and indentation mapping as a readily accessible means of probing the surface features of heterogeneous surfaces.

### Experimental Section

The synthesis of poly(dodecyl methacrylate), PDDMA, has been described elsewhere;<sup>13</sup> poly(methyl methacrylate), PMMA was obtained from Goodfellow (Cambridge, U.K.). Films of the polymer blend were deposited onto glass slides (8 mm × 8 mm × 1 mm) by immersion into a stirred solution (2.5% w/w) of PDDMA and PMMA (1:1 (w/w) PDDMA/PMMA) in chloroform; films for AFM work were rinsed with ethanol (Analar, BDH). A TopoMetrix TMX2000 discoverer scanning probe microscope (ThermoMicroscopes, Bicester, U.K.) was employed for both topographic imaging and force measurements. For adhesion studies, V-shaped, silicon nitride cantilevers (200 μm in length; nominal spring constant,  $K$ , 0.032 N m<sup>-1</sup>; part Nno. 1520-00; ThermoMicroscopes, Santa Clara, CA) were used. Since the actual spring constant of the V-shaped commercial cantilevers is known to differ by up to an order of magnitude from the nominal value,<sup>14</sup> the  $K$  value associated with each cantilever was determined using an established procedure.<sup>13</sup> Indentation measurements were made using beam-shaped silicon cantilevers (length = 231 μm, width = 37 μm, thickness = 6.7 μm;  $K$  = 38 N m<sup>-1</sup>; nanosensors, LOT Oriel Ltd, Leatherhead U.K.). Topographic imaging was performed in contact mode, both in air (ambient conditions) and under water (using a wet cell). Layered imaging was used to obtain force–distance curves over an entire image frame of 10 μm × 10 μm at a resolution of 50 lines × 50 pixels (2500 force curves) for adhesion imaging, and 100 lines × 100 pixels (10000 force curves) for indentation imaging;<sup>5</sup> the scan rate was 1 μm s<sup>-1</sup>. For each layered image acquired, a corresponding topographic image of identical resolution and spatial orientation was also obtained. Layered images were obtained under ambient conditions or under dry nitrogen in a gas cell (relative humidity <1% as measured using a hygrometer; model HI 91610C, Hanna Instruments, Leighton Buzzard, U.K.); a slight positive pressure was maintained throughout the experiments.

The adhesion maps were extracted from layered images using an algorithm, which was designed to remove contributions from topography; the program (Visual Basic) plotted the adhesion force values as a gray-scale image. For indentation measurements, a program facilitated the calculation of the extent of the surface indentation of the sample—caused by the probing tip—relative to a stiff reference material (stainless steel AISI 304), such that the contribution to deflection due to cantilever bending was eliminated. After contact with the surface was established, an arbitrary point along the inward force curve was used to demarcate cantilever deflection. Indentation was plotted as a gray-scale image, with lighter shades representing greater indentation.

### Results and Discussion

A typical topographic image of the surface of the PDDMA/PMMA blend, Figure 1, reveals a binary structure with multiple raised (light) and lowered (dark) domains. The line profile across this image shows that the height

\* Corresponding author: tel ++44 (0)2392 84 3606; fax ++44 (0)2392 84 8879; e-mail john.tsibouklis@port.ac.uk.

(1) Binnig, G.; Quate, C. F.; Gerber, C. *Phys. Rev. Lett.* **1986**, *56*, 930–933.

(2) Cappella, B.; Dietler, T. *Surf. Sci. Rep.* **1999**, *34*, 1–104.

(3) Mizes, H. A.; Loh, K. G.; Miller, R. J. D.; Ahuja, S. K.; Grabowski, E. F. *Appl. Phys. Lett.* **1991**, *59*, 2901–2903.

(4) Krottil, H.-U.; Stifter, T.; Marti, O. *Appl. Phys. Lett.* **2000**, *77*, 3857–3859.

(5) Eaton, P.; Graham, P.; Smith, J. R.; Smart, J. D.; Nevell, T. G.; Tsibouklis, J. *Langmuir* **2000**, *16*, 7887–7890.

(6) Weisenhorn, A. L.; Maivald, P.; Butt, H. J.; Hansma, P. K. *Phys. Rev. B: Condens. Matter Mater. Phys.* **1992**, *45*, 11226–11232.

(7) Beake, B. D.; Brewer, N. J.; Leggett G. J. *Macromol. Symp.* **2001**, *167*, 101–115.

(8) Burnham, N. A.; Colton, R. J. *J. Vac. Sci. Technol., A* **1989**, *7*, 2906–2913.

(9) Raghavan, D.; Gu, X.; Nguyen, T.; Vanlandingham, M.; Karim, A. *Macromolecules* **2000**, *33*, 2573–2583.

(10) Penegar, I.; Toque, C.; Connell, S. D. A.; Smith, J. R.; Campbell, S. A. *Additional Papers From the 10th. International Congress on Marine Corrosion and Fouling* 2001.

(11) Xu, W.; Mulhern, P. J.; Blackford, B. L.; Jericho, M. H.; Templeton, I. *Scanning Microsc.* **1994**, *8*, 499–506.

(12) Vinckier, A.; Semenza, G. *FEBS Lett.* **1998**, *430*, 12–16.

(13) Tsibouklis, J.; Graham, P.; Peters, V.; Eaton, P.; Smith, J. R.; Nevell, T. G.; Smart, J. D.; Ewen, R. J. *Macromolecules* **2000**, *33*, 8460–8465.

(14) Cleveland, J. P.; Manne, S.; Bocek, D.; Hansma, P. K. *Rev. Sci. Instrum.* **1993**, *64*, 403–405.

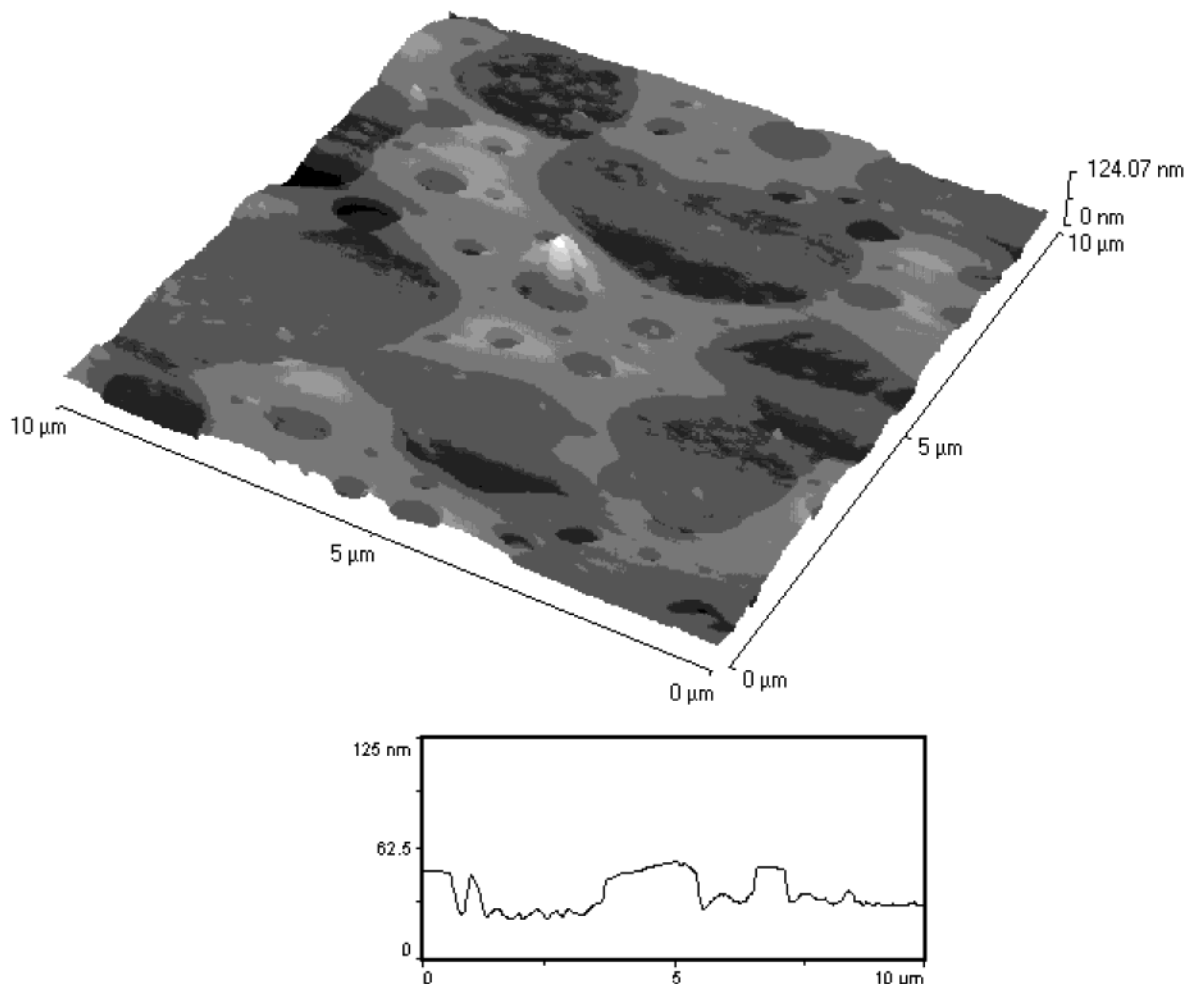


**Figure 1.** Typical contact-mode AFM topography image of the PMMA/PDDMA blend film (top) and a typical surface roughness profile across the same image (bottom). The height difference between the PDDMA-rich and the PMMA-rich domains is ca. 25 nm.

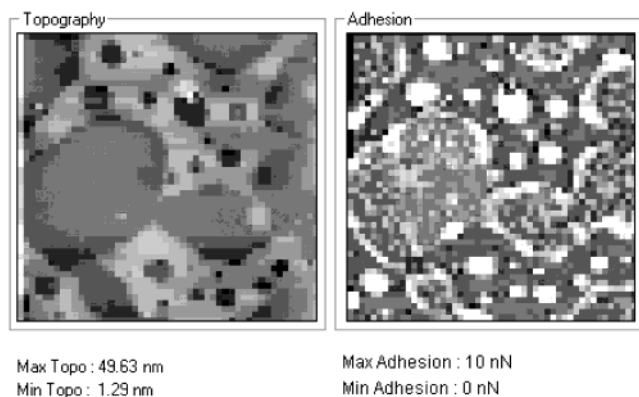


**Figure 2.** Topography and adhesion maps ( $10\ \mu\text{m} \times 10\ \mu\text{m}$ ) of the PMMA/PDDMA blend film. Lighter shades are used to represent raised features in the topographic image (left) or augmented forces in the adhesion map (right).

difference between the two types of domain was typically ca. 25 nm. An adhesion map of this sample, obtained under dry conditions, Figure 2, shows variations corresponding closely with the topography. Interestingly, the interface between the two polymer domains is highlighted as a region of extreme adhesive interactions; a bright halo with a dark periphery is demarcating the domain boundaries. Consideration of the effect of topography on the proximal AFM tip provides an explanation for the origins of this feature: when the tip is close to a vertical face of an elevated domain, the substrate surface area interacting

with the tip increases, resulting in an enhancement in the measured force of adhesion. By similar reasoning, closely associated areas of low adhesion (dark) may be attributed to the sharply convex surface features witnessed in the topographic line profile, Figure 1. The presence of such features highlights the complementary nature of force-of-adhesion measurements and topographic imaging in the study of multidomain structures.

As a test for our hypothesis regarding the effects of increased contact area on measured force of adhesion, a scratched commercial sample of PMMA was subjected to adhesion force mapping, in the expectation that any contrast seen in the adhesion force images would be due to the effects of topography; relatively smooth ( $R_a = 3.8\ \text{nm}$ ) films of pure polymers are associated with featureless adhesion-map images. In corresponding topography and adhesion maps, Figure 3, both the pits, inherent to the surface of the sample, and the interpolated scratches are visualized as lines of high adhesion bounded by low adhesion, thus providing support for the hypothesis. Since the image shown in Figure 2 was obtained under dry conditions, capillary-water-layer effects, such as those recently highlighted by Sirghi et al.,<sup>15</sup> could not have been of influence. On the basis of the topographic image alone, it could be assumed that the two domains visible in Figure 1 correspond to pure PMMA and PDDMA, respectively. However, the adhesion map presented in Figure 2 suggests

(15) Sirghi, L.; Nakagiri, N.; Sugisaki, K.; Sugimura, H.; Takai, O. *Langmuir* **2000**, *16*, 7796–7800.

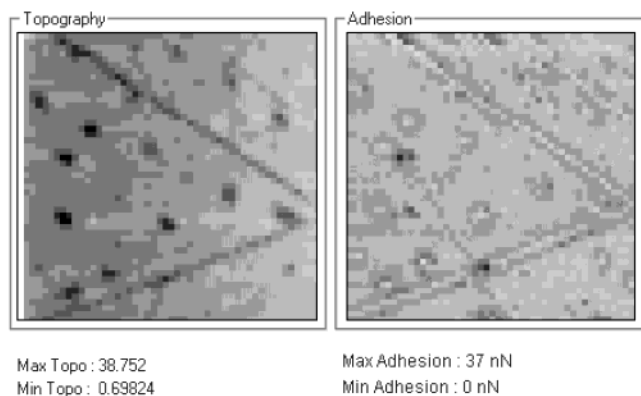


**Figure 3.** Topography (left) and adhesion (right) maps ( $10\ \mu\text{m} \times 10\ \mu\text{m}$ ) of a scratched PMMA surface. The scratches are seen as the darker lines in the topographic image or as the lighter lines in the adhesion map.

that the additional, submicrometer-scale features observed within each domain arise as a result of the presence of varying proportions of the minor polymeric constituent.

The complementary contribution of indentation mapping (with corresponding topography) to the study of multidomain structures is highlighted in Figure 4, which is representative of a series of cantilever deflection measurements at individual pixel positions, each obtained with the same constant applied load (61 nN). The nanoindentation maps highlight the submerged, high indentation regions (bright) as those of the more yielding, PDDMA-rich domains, a diagnosis not possible by topographic imaging or force-of-adhesion mapping alone. In view of the difficulties associated with the estimation of Young's modulus using nanoindentation techniques<sup>11</sup> and the fact that the value of Young's modulus for PDDMA is not available in the literature, no attempt was made to quantify the stiffness of the probed sample. Comparison of the indentation map (Figure 4) with the adhesion image (Figure 2) provides support for the hypothesis that the AFM-determined adhesion behavior of these polymeric materials may be due to the increased area of interaction between the tip and the probed surface, resulting from physical deformation of, or damage to, the polymer surface. Characteristically, indentation mapping—in contrast with adhesion mapping—does not appear to be influenced by

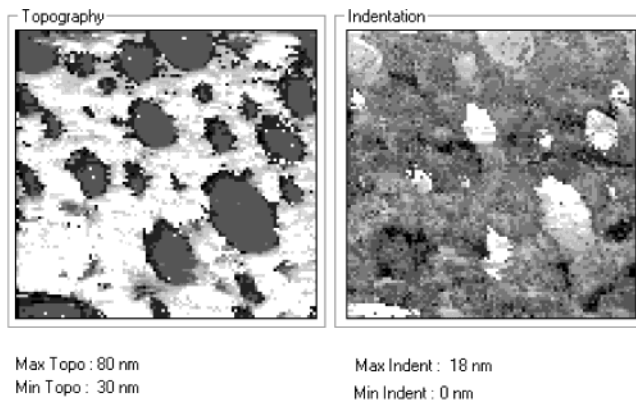


**Figure 4.** Topography and indentation maps ( $10\ \mu\text{m} \times 10\ \mu\text{m}$ ) of the PDDMA/PMMA blend film. Lighter shades are used to highlight elevated features (left) or increased ease of indentation (right)—these correspond to PDDMA-rich domains. The indentation map was obtained using an applied load of 61 nN.

topographic features. This can probably be explained in terms of tip sharpness: tips used for nanoindentation measurements are sharper (tip radius  $< 20\ \text{nm}$ ) than those employed for the adhesion work (tip radius  $< 40\ \text{nm}$ ).

### Conclusions

The AFM techniques of adhesion force mapping and indentation mapping have been applied to the examination of the topographic features of a polymer blend. Adhesion maps have revealed that particularly high adhesion forces operate at the boundaries between domains. Complementary data from the two techniques have shown that these forces derive from the increased contact area between the probing tip and the sample. In addition, the work revealed that high adhesion areas are more susceptible to indentation by the data collecting action of the AFM probe, further suggesting that sample indentation may amplify the force-of-adhesion values obtained from easily indented samples.

**Acknowledgment.** The authors wish to thank the EPSRC (Peter Eaton) and NERC (Paul Graham) for supporting this work.

LA015633L